

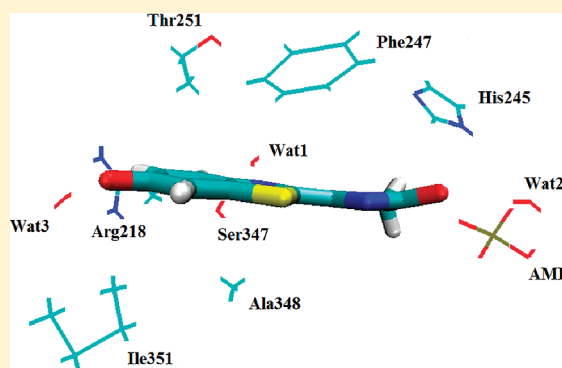
TD-DFT/Molecular Mechanics Study of the *Photinus pyralis* Bioluminescence System

Luís Pinto da Silva and Joaquim C. G. Esteves da Silva\*

Centro de Investigação em Química (CIQ-UP), Departamento de Química e Bioquímica, Universidade do Porto, Porto, Portugal

## S Supporting Information

**ABSTRACT:** This is the first report of a computational study of the bioluminescence of ligand-bound *Photinus pyralis* luciferase. A time-dependent PBE0/molecular mechanics approach was used to study the interaction between excited-state oxyluciferin (Keto-(−1)) and neighboring active site molecules. The results of these calculations demonstrated that the most important intermolecular interactions are: blue-shifting ionic interactions, red-shifting  $\pi$ - $\pi$  stacking, and red/blue shifting hydrogen bonding. Subsequent molecular dynamics simulations further supported these conclusions.



## ■ INTRODUCTION

Bioluminescence is a light-emitting phenomenon that occurs in living organisms, in which an excited-state molecule is produced in a luciferase-catalyzed reaction.<sup>1</sup> The most studied bioluminescence system is that of the North American firefly, *Photinus pyralis*.<sup>1</sup> Firefly luciferase (Luc, EC 1.13.12.7) catalyzes a two-step reaction: first, it catalyzes the formation of an adenylyl intermediate, from firefly luciferin (LH<sub>2</sub>) and adenosine-5'-triphosphate (ATP); in the second step, that intermediate is oxidized, in the presence of molecular oxygen, into oxyluciferin (OxyLH<sub>2</sub>).<sup>1</sup> This molecule has a great importance in this system, as besides being the light emitter, it appears to be one of the major responsible for the flash profile of the emitted light.<sup>1–5</sup> In more recent years, the bioluminescence phenomenon has received attention from the research community and has gained numerous biomedical, pharmaceutical, and bioanalytical applications. More specifically, it is involved in the analytical determination of ATP, in microbial detection, biosensing, and bioimaging, and is used as a gene reporter.<sup>6–10</sup>

One of the most studied and elusive aspects of firefly bioluminescence is its multicolor emission.<sup>11</sup> Luc is a pH-sensitive enzyme, and at basic pH (pH  $\approx$  7.5) the emission has a peak at 562 nm. At acid pH (pH  $\approx$  5–6), the emission shifts to the red region of the visible spectrum, with a maximum at 620 nm.<sup>11</sup> The understanding of this feature could be used to improve the efficiency of Luc-based applications. Lower energy emitting Luc could be used in the in vivo medical imaging, as red light is absorbed very poorly in comparison with natural emitted light. Viviani et al. also hypothesized that the control of the multicolor emission could be applied in the use of Luc as a single dual reporter gene, as a bioindicator of cellular stress, and as a probe for intracellular changes of pH.<sup>12</sup> Numerous authors

have tried to explain this natural phenomenon. The indication and analysis of all of the experimental and theoretical contributions for this topic can be found in these four recent reviews.<sup>11,13–15</sup>

For a correct description of the bioluminescence phenomenon, an exact identification of the luminophore is needed. The identification of Keto-(−1) (Figure 1) as the light emitter was

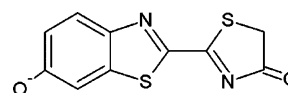


Figure 1. Schematic representation of Keto-(−1).

only achieved rather recently, by analysis of the dissociation and tautomeric constants of OxyLH<sub>2</sub> as a function of pH, by the study of the direct excited-state product of firefly dioxetanone, and by the study of the possibility of keto–enol tautomerism in *Luciola cruciata* Luc (LcLuc) active site.<sup>16–18</sup> However, it should be stressed that all of these studies are theoretical, and until now no experimental study has conclusively defined Keto-(−1) as the sole light emitter.

One of the most fundamental studies in this field of research was the determination of the crystal structure of LcLuc.<sup>19</sup> This experimental work indicated that LcLuc is capable of assuming different conformations during the various stages of the bioluminescence reaction. Thus, the complex of LcLuc with an adenylyl intermediate analogue presented a more hydrophobic and closed active site, while in the case of the enzyme-

Received: December 13, 2011

Revised: January 14, 2012

Published: January 14, 2012

OxyLH<sub>2</sub>-adenosine-5'-monophosphate (AMP) complex a more open and polar active site was found. Because of the fact that a red-emitting LcLuc mutant only presents the second conformation, it was hypothesized by the authors that the more closed conformation could be responsible for green emission, and the more open one for red emission.<sup>19</sup>

In some previous Time-Dependent Density Functional Theory (TD-DFT)-based studies, some authors have tried to analyze the effect of various small molecules and of polarity in the multicolor emission of OxyLH<sub>2</sub>.<sup>16,20–24</sup> These calculations demonstrated that the color of light by Keto(–1) can be modulated by the type of intermolecular interactions that the luminophore may form with other molecules. Furthermore, the polarity of the microenvironment has also an effect in the emission maxima. On the basis of these findings, we have studied the effect on intermolecular interactions and polarity in the multicolor bioluminescence. To this end, we have docked excited-state Keto(–1) to both conformations of LcLuc and have analyzed the different effects exerted by active site molecules on emission.<sup>24,25</sup> We have then stated that a red-shift can be achieved by modification of the hydrogen-bond network, and changes in the electrostatic and  $\pi$ – $\pi$  stacking interactions between Keto(–1) and AMP and Phe249, respectively. These conclusions are in line with both theoretical and experimental works from other researchers.<sup>26–30</sup> More recently, Song and Rhee developed some new force field parameters for both the ground and the excited states of Keto(–1).<sup>16,31</sup> Also, they have demonstrated the importance of taking into account the environmental dynamics in the study of the multicolor bioluminescence. Moreover, they have stated that the most important factor, in the color tuning mechanism, is the electrostatic interactions between the luminophore and neighboring molecules. Thus, this conclusion devalues the importance of other types of intermolecular interactions and contradicts the results of other authors.

The purpose of this Article is to study, for the first time, the bioluminescence phenomenon in the more closed and hydrophobic active site of *Photinus pyralis* Luc (PDB ID: 3IES).<sup>32</sup> It should be noted that, while Nakatani et al. also have tried to study theoretically the bioluminescence of *Photinus pyralis* Luc, they have used a structure derived from unbound Luc and a working model.<sup>30</sup> Therefore, their structure may have significant differences regarding the crystal structure of bound Luc, here computationally studied for the first time. To this end, we have docked excited-state Keto(–1) to the active site of Luc in the closed conformation, by means of protein–ligand docking. The Luc–emitter complex was minimized by using molecular mechanics (MM). Subsequently, the emitters and some chosen active site molecules were withdrawn from the resulting structure. Theoretical calculations on these models demonstrated the effect of these static active site molecules in the emission of Keto(–1). Finally, molecular dynamics (MD) simulations were performed to study the effect of environmental dynamics in the bioluminescence phenomenon. Thus, our approach will enable the expansion of the bioluminescence research to ligand-bounded crystal structures other than LcLuc, and the study of the luminophore–active site interactions as a function of time.

The results achieved in this Article demonstrated that the intermolecular interactions that are fundamental to the color tuning mechanism are ionic interactions,  $\pi$ – $\pi$  stacking, and hydrogen bonding. These results are in line with previous experimental and theoretical bioluminescence stud-

ies.<sup>18,25–28,30,33</sup> Also, it was demonstrated that the inclusion of dynamic features affects quantitatively (but not qualitatively) the emission wavelength of Keto(–1) and Keto(–1)–X complexes. The present and some previous results validate the hypothesis that there are intermolecular interactions that modulate the color of bioluminescence, as they have a similar effect on the emission of Keto(–1) in different firefly species.<sup>25</sup>

## ■ COMPUTATIONAL METHODS

The PDB structure 3IES was used as starting structure, in the study of the bioluminescence of Keto(–1). The hydrogens atoms, the missing atoms, and TIP3P water molecules up to 12 Å were added by the LEAP module of the AMBER 11 suite of programs.<sup>34</sup> The ff03 force field was used for intramolecular interactions.<sup>35</sup> The ground-state geometries of AMP and Keto(–1) were calculated at the HF/6-31G(d) level of theory.<sup>36</sup> The configuration interaction singles (CIS) functional, with the 6-31G(d) basis set, was used to calculate the first singlet ( $S_1$ ) excited-state geometry of Keto(–1).<sup>37</sup> The CIS method was chosen as Nakatani et al. demonstrated that it is comparable to methods of higher levels of theory.<sup>30</sup> The ground-state structure of AMP and the excited-state geometries of Keto(–1) were used in their parametrization with the ANTECHAMBER module of AMBER and the general AMBER force field.<sup>38</sup> These two molecules were docked to the active site by use of the software AUTODOCK 4.2.<sup>39</sup> The genetic algorithm was used as a search engine.

One phase of energy minimization (30 000 steps) was performed, using the Not (just) Another Molecular Dynamics program (NAMD) molecular dynamic code with AMBER potential functions, parameters, and the file formats.<sup>40</sup> All of the minimizations steps were performed in a NVT ensemble, with a temperature of 298.15 K. In this process, the Particle Mesh Ewald method was used to include the long-range interactions.<sup>41</sup> In the end of the energy minimizations, Keto(–1) was withdrawn from the resulting structures along with Arg218, His245, Phe247, Thr251, Ser347, Ala348, Ile351, AMP, and three water molecules. Because of the high number of atoms involved, only the interacting side chains of the amino acids and the phosphate group of AMP were considered in the calculations, as can be seen in Figure 1 of the Supporting Information. These molecules were chosen on the basis of previous computational studies on LcLuc, to detect possible differences and similarities between the color tuning mechanism of the two enzymes.<sup>18,19,22,25,26,30</sup> All of the active site molecules were within 6 Å from Keto(–1).

MD simulations were performed with NAMD, on the MM-minimized system composed by Luc, AMP, Keto(–1), and water molecules up to 12 Å. These coordinates were used in a MD simulation of 500 ps, at 298.15 K. Nonbonded interactions were considered with 14 Å cutoffs. The integration step size was 2 fs, and all bonds involving hydrogen and heavy atoms were constrained.

The emission wavelengths of Keto(–1) and respective complexes with active site molecules were computed at the time-dependent (TD) PBE0/6-31+G(d) level of theory, with solvent effects.<sup>42–44</sup> Despite some critics to the use of TD-DFT in bioluminescence research due to errors regarding charge transfer (CT) states, the work of Li et al. showed us that CT is small on planar OxyLH<sub>2</sub>, thus devaluing this flaw of TD-DFT methods.<sup>45–47</sup> The complexes that resulted from both the MM and MD simulations were used in the TD-DFT calculations

without further optimization. To simulate the polarity of the active site of Luc, the conductor-like polarized continuum model (CPCM) was used to treat the effects due to bulk solvent.<sup>48</sup> The dielectric constant of 4 was used to simulate the hydrophobic environment of the active site. All HF/CIS/TD-DFT calculations were performed with the Gaussian 03 program package.<sup>49</sup>

## RESULTS AND DISCUSSION

**Analysis of the Static Interaction between Keto(-1) and Active Site Molecules.** In Table 1 are indicated the

**Table 1.** Calculated Emission Wavelength ( $\lambda_{\text{max}}$  in nm) of Keto(-1) and Keto(-1)-X Complexes<sup>a</sup>

	$\lambda_{\text{max}}$	$\Delta\lambda_{\text{max}}$
Keto(-1)	528	
Keto(-1)-Arg218	521	7
Keto(-1)-His245	531	-3
Keto(-1)-Phe247	531	-3
Keto(-1)-Thr251	528	0
Keto(-1)-Ser347	529	-1
Keto(-1)-Ala348	528	0
Keto(-1)-Ile351	531	-3
Keto(-1)-AMP	501	27
Keto(-1)-Wat1	538	-10
Keto(-1)-Wat2	537	-9
Keto(-1)-Wat3	516	12

<sup>a</sup>In the third column are indicated the difference between the emission wavelength of Keto(-1) and Keto(-1)-X ( $\Delta\lambda_{\text{max}}$  in nm). Positive values correspond to blue-shifting contributions, while negative values refer to red-shifting ones.

wavelength maxima of excited-state Keto(-1), when interacting with each one of the active site molecules and without directly interacting with that molecule. In Figure 2 are

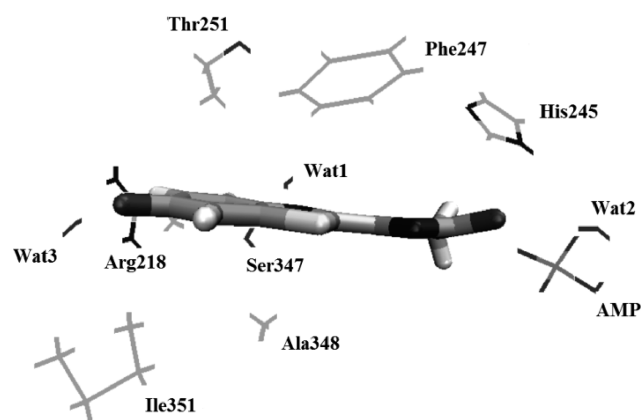


**Figure 2.** Representation of the complex between Keto(-1) and active site molecules.

represented Keto(-1) and surrounding active site molecules. When in comparison with the active site of LcLuc, the major difference is that Keto(-1) is interacting with three water molecules (with the benzothiazole/thiazolone oxygen and the benzothiazole nitrogen) at the same time.

As was already expected due to our previous studies, Table 1 results demonstrate that ionic interactions blue-shift the emission.<sup>16,21,22</sup> Positively charged Arg218 and negatively

charged AMP both decrease the emission of Keto(-1), with different extents. The calculated blue-shifting contribution of AMP differs by 20 nm from the contribution of Arg218.

Our analysis also reveals that the polarization of the benzothiazole moiety, made here by Ser347, has a small red-shifting contribution as in the case of LcLuc.<sup>25</sup> The polar Thr251 has no effect in the emission, also as in the case of LcLuc.<sup>25</sup> Ala348 also does not modulate the color of light emitted by the emitter. The also hydrophobic molecule Ile351 red-shifts the emission of Keto(-1). Phe247 presents opposite contribution in Luc than its corresponding phenylalanine residue in LcLuc closed conformation, by red-shifting the emission of Keto(-1).<sup>25</sup> His245, as Phe247, is a red-shifting molecule.

Analysis of Table 1 also demonstrated the importance of the hydrogen-bond network in the tuning of the emission of Keto(-1), as all three water molecules gave importance contributions to the wavelength maxima. Wat3 interacts with the benzothiazole oxygen, thereby decreasing its emission wavelength by 12 nm.<sup>19-21</sup> Wat1 and Wat2 interact with the thiazole and the thiazolone moieties, respectively, which leads to increased emission wavelengths.<sup>16,20-22,25</sup>

In conclusion, we can state that the most important blue-shifting interactions are ionic interactions (AMP and Arg218) and hydrogen bonding with the benzothiazole oxygen (Wat3). The most important red-shifting interactions are  $\pi$ -interactions (Phe247) and hydrogen bonding with the thiazole/thiazolone moieties (Wat1 and Wat2). The effect of hydrophobic interactions (Ile351 and Ala348) and polarization of the benzothiazole microenvironment (Thr251 and Ser347) appears to be less important, as indicated in previous studies.<sup>16,20,25</sup> Also, we can state that our decision of modeling the active site molecules, as represented in Figure 1 of the Supporting Information, does not affect this study as the values found here are similar to those calculated in the case of LcLuc with full active site molecules.<sup>25</sup>

**MD Simulation Regarding Excited-State Keto(-1)-Luc Complex.** In Table 2 are represented the emission

**Table 2.** Calculated Emission Wavelength ( $\lambda_{\text{max}}$  in nm) of Keto(-1) and Keto(-1)-X Complexes, at 125, 250, 375, and 500 ps (ps) of MD Simulation

	$\lambda_{\text{max}}$			
	125 ps	250 ps	375 ps	500 ps
Keto(-1)	518	538	545	561
Keto(-1)-Arg218	514	535	541	556
Keto(-1)-His245	526	541	548	565
Keto(-1)-Phe247	522	543	556	566
Keto(-1)-Thr251	519	538	545	561
Keto(-1)-Ser347	520	539	546	563
Keto(-1)-Ala348	518	538	545	561
Keto(-1)-Ile351	521	539	546	564
Keto(-1)-AMP	495	511	522	538
Keto(-1)-Wat1	528	546	555	573
Keto(-1)-Wat2	524	545	545	577
Keto(-1)-Wat3	507	525	534	544

wavelengths of sole Keto(-1) and Keto(-1) complexed with one active site at 125, 250, 375, and 500 ps of the MD simulation. In Table 3 are represented the red- or blue-shifting contribution of the active site molecules to the emission of Keto(-1), in the form of the difference between the emission



**Table 3. Calculated Difference between the Emission Maxima of Keto-(−1) ( $\Delta\lambda_{\text{max}}$  in nm) and Keto-(−1)–X Complexes, at 125, 250, 375, and 500 ps (ps) of MD Simulation<sup>a</sup>**

	$\Delta\lambda_{\text{max}}$			
	125 ps	250 ps	375 ps	500 ps
Keto-(−1)–Arg218	4	3	4	5
Keto-(−1)–His245	−8	−3	−3	−4
Keto-(−1)–Phe247	−4	−5	−11	−5
Keto-(−1)–Thr251	−1	0	0	0
Keto-(−1)–Ser347	−2	−1	−1	−2
Keto-(−1)–Ala348	0	0	0	0
Keto-(−1)–Ile351	−3	−1	−1	−3
Keto-(−1)–AMP	23	27	23	24
Keto-(−1)–Wat1	−10	−8	−10	−12
Keto-(−1)–Wat2	−6	−7	0	−16
Keto-(−1)–Wat3	11	13	11	17

<sup>a</sup>Positive values correspond to blue-shifting contributions, while negative values refer to red-shifting ones.

wavelength of Keto-(−1) and the emission maxima of Keto-(−1)–X complexes. It should be stated that, while Wat1 and Wat3 are hydrogen-bonded to Keto-(−1) during the period of the simulation, the bond between Wat2 and Keto-(−1) is broken in some points of the simulation. This breaking thereby explains the contribution of 0 nm of Wat2, at 375 ps of the MD simulation.

As was already noticed by Song and Rhee, the inclusion of a dynamic component in the calculations has an effect on the bioluminescence of Keto-(−1).<sup>18</sup> As can be seen by comparing Tables 1 and 2, the emission maxima computed at different periods of the MD simulation are all blue- or red-shifted as compared to the maxima calculated for the MM energy minimizations. However, the trends regarding the effect of intermolecular interaction in the emission remain the same.

Ala348 and Thr251 still have a zero contribution in the emission of Keto-(−1). Arg218 and AMP still behave as blue-shifting molecules. However, AMP blue-shifts the emission by 23–27 nm, while Arg218 only has a small contribution to the emission of Keto-(−1). This large effect indicates that AMP is one of the most important molecules in the color tuning mechanism, as stated in previous studies.<sup>18,25,27</sup>

Both Ile351 and Ser347 have small red-shifting contributions to the emission. These data further support previous results, which indicate that the polarization of the benzothiazole moiety, and hydrophobic interactions with that same moiety, red-shift the emission.<sup>20,25,26</sup>

As was already indicated both by theory and by experiment,  $\pi$ – $\pi$  stacking interaction is a key factor in the color tuning mechanism. Phe247 is one of the most important red-shifting molecules, with contributions as high as 11 nm. This importance is also seen in LcLuc.<sup>25</sup> His245 is also of some importance, with red-shifting contributions as high as 8 nm.

The hydrogen-bond network appears also to be of great importance in the color tuning mechanism. Wat3 is an important blue-shifting molecule, with a steady contribution of 11–17 nm. Wat1 and Wat2 are also molecules that are fundamental for the multicolor bioluminescence, by increasing the emission wavelength of Keto-(−1). Wat1 appears to be the more important of the two water molecules, by presenting higher red-shifting contributions. Furthermore, this molecule is hydrogen bonded to Keto-(−1) during the 500 ps of the

simulation, while Wat2 has no interaction with the light emitter in some points (as exemplified at 375 ps of simulation). These results further support some previous studies, which demonstrated that some types of intermolecular interactions (as hydrogen bonding) have opposite effects, if made with the benzenic or with the thiazole/thiazolone moieties.<sup>20,25</sup>

Thus, the results here presented support our working hypothesis, which states that the multicolor bioluminescence is achieved by modulation of the color of light by intermolecular interactions.<sup>16,20,25</sup> Furthermore, this study allows us to clearly define the most important type of the intermolecular interactions: ionic,  $\pi$ – $\pi$  stacking, and hydrogen bonding. The conclusions of this Article gain more strength, as they support the conclusions achieved for other firefly species (*Luciola cruciata*).<sup>25</sup> Therefore, this indicates that we have defined a mechanism for the multicolor bioluminescence that can be found in different species of firefly, with similar results, as seen experimentally.<sup>12</sup> Also, the importance of performing dynamic simulations in the study of the multicolor bioluminescence (as stated by Song and Rhee)<sup>18</sup> was corroborated.

To try to understand the effect of intermolecular interactions in color modulation, we have calculated the energy of the excited state of Keto-(−1) complexed with Phe247, AMP, or Wat1. All three complexes suffer from a red-shift, with increasing time in the MD simulation. Therefore, it was expected that the excited state would be more stabilized during the course of the calculations. However, as can be seen in Table 4, there is no stabilization of the excited state with increasing

**Table 4. Energy Levels (in hartrees) of the Ground and Excited States of Keto-(−1)–Phe247, Keto-(−1)–AMP, and Keto-(−1)–Wat1, at 125, 250, 375, and 500 ps (ps) of the MD Simulation**

Keto-(−1)–Phe247				
	125 ps	250 ps	375 ps	500 ps
excited state	−1671.391	−1671.391	−1671.390	−1671.377
ground state	−1671.478	−1671.475	−1671.472	−1671.458
Keto-(−1)–AMP				
	125 ps	250 ps	375 ps	500 ps
excited state	−2082.087	−2082.079	−2082.090	−2082.073
ground state	−2082.179	−2082.168	−2082.178	−2082.158
Keto-(−1)–Wat1				
	125 ps	250 ps	375 ps	500 ps
excited state	−1515.783	−1515.775	−1515.779	−1515.765
ground state	−1515.870	−1515.859	−1515.861	−1515.845

emission wavelength. Thus, as emission wavelength depends also on the ground state, we have computed the energy level of this state for all three complexes. Similarly to the excited state, there is no destabilization of the ground state with decreasing emission energies. However, an approximation of the energy level between both states can be seen for all complexes, indicating that intermolecular interactions modulate the color of emission, not by stabilizing/destabilizing one of the states but by affecting both the excited and the ground states.

A final note should be made regarding the study of Roca-Sanjuán et al., published after we performed the calculations here presented.<sup>50</sup> The authors state that the more appropriate strategy for modeling correctly the bioluminescence state is to use a peroxo intermediate as the starting structure, while it is

common to start by the ground-state optimized structure of the reaction product (as performed here). However, other authors who also did not describe their modeling of Keto(−1) as starting with the peroxo intermediate achieved results that agree very well with experiment.<sup>18,26</sup> Therefore, the impact of the recommendation of Roca-Sanjuán et al., in the bioluminescence research, needs further assessing.<sup>50</sup>

## CONCLUSIONS

We have employed various computational methodologies to study the color tuning mechanism behind the multicolor bioluminescence. By using for the first time the crystal structure of the closed conformation of *Photinus pyralis* Luc, we have studied the interaction of Keto(−1) with active site molecules.

Our calculations demonstrated that the most important types of intermolecular interactions are: blue-shifting ionic interactions (with AMP), red-shifting  $\pi$ – $\pi$  stacking (with Phe247), and red/blue-shifting hydrogen bonding (with Wat1/2/3). Amino acids Arg218 and His245 present smaller but also important blue- and red-shifting contributions, respectively, while Ser347, Ile351, Thr251, and Ala348 appear to be irrelevant in the color tuning mechanism. Thus, these molecules may be good targets to amino acids mutations, with the objective of modulating the emission wavelength.

We have also performed molecular dynamics simulations with the Luc–emitter complex. Analysis of the results supported the conclusions derived from the study of the static Luc–Keto(−1) complex. Furthermore, this study (along with our previous studies) demonstrated that the key role of intermolecular interactions can be seen in different firefly species, as in the presence or absence of dynamic features.

Analysis of the energy levels of both the ground and the excited states of three different Keto(−1)–X complexes revealed the mechanism in which intermolecular interactions tune the color of emission. There is no stabilization/destabilization of a single state, but rather a stabilization/destabilization of both states. Thus, red- or blue-shifts are achieved by approximating or spacing between the energy levels of the ground and excited states, respectively.

## ASSOCIATED CONTENT

### Supporting Information

Schematic representation of the active site molecules studied in this Article, and Cartesian coordinates of the excited-state geometry of Keto(−1) used for its parametrization and of the MM-resulting complex between Keto(−1) and the modified active site molecules. This material is available free of charge via the Internet at <http://pubs.acs.org>.

## AUTHOR INFORMATION

### Corresponding Author

\*Tel.: (+351) 220-402-569. Fax: (+351) 220-402-659. E-mail: [jcsilva@fc.up.pt](mailto:jcsilva@fc.up.pt).

### Notes

The authors declare no competing financial interest.

## ACKNOWLEDGMENTS

Financial support from Fundação para a Ciência e Tecnologia (FCT, Lisbon) (Programa Operacional Temático Factores de Competitividade (COMPETE) e participado pelo Fundo Comunitário Europeu FEDER) (Project PTDC/QUI/71366/

2006) is acknowledged. A Ph.D. grant to L.P.d.S. (SFRH\BD\76612\2011), attributed by FCT, is also acknowledged.

## REFERENCES

- (1) Marques, S. M.; Esteves da Silva, J. C. G. *IUBMB Life* **2009**, *61*, 6–17.
- (2) Esteves da Silva, J. C. G.; Magalhães, J. M. C. S.; Fontes, R. *Tetrahedron Lett.* **2001**, *42*, 8173–8176.
- (3) Ribeiro, C.; Esteves da Silva, J. C. G. *Photochem. Photobiol. Sci.* **2008**, 1085–1090.
- (4) Leitão, J. M.; Esteves da Silva, J. C. G. *J. Photochem. Photobiol.* **2010**, *101*, 1–8.
- (5) Pinto da Silva, L.; Esteves da Silva, J. C. G. *Photochem. Photobiol. Sci.* **2011**, *10*, 1039–1045.
- (6) Roda, A.; Pasini, P.; Mirasoli, M.; Michelini, E.; Guardigli, M. *Trends Biotechnol.* **2004**, *22*, 295–303.
- (7) Luker, K. E.; Luker, G. D. *Antiviral Res.* **2008**, *78*, 179–187.
- (8) Fan, F.; Wood, K. V. *Assay Drug Dev. Technol.* **2007**, *5*, 127–136.
- (9) Branchini, B. R.; Southworth, T. R.; Khattak, N. F.; Michelini, E.; Roda, A. *Anal. Biochem.* **2005**, *345*, 140–148.
- (10) Doyle, T. C.; Burns, S. M.; Contag, C. H. *Cell Microbiol.* **2004**, *6*, 303–317.
- (11) Pinto da Silva, L.; Esteves da Silva, J. C. G. *J. Chem. Theory Comput.* **2011**, *7*, 809–817.
- (12) Viviani, V. R.; Arnoldi, F. G. C.; Neto, A. J. S.; Oehlmeyer, T. L.; Bechara, E. J. H.; Ohmiya, Y. *Photochem. Photobiol. Sci.* **2008**, *7*, 159–169.
- (13) Hosseinkhani, S. *Cell. Mol. Life Sci.* **2011**, *68*, 1167–1182.
- (14) Hasegawa, J. Y.; Fujimoto, K. J.; Nakatsuji, H. *ChemPhysChem* **2011**, *12*, 3106–3115.
- (15) Navizet, I.; Liu, Y. J.; Ferré, N.; Roca-Sanjuá, D.; Lindh, R. *ChemPhysChem* **2011**, *12*, 3064–3076.
- (16) Pinto da Silva, L.; Esteves da Silva, J. C. G. *ChemPhysChem* **2011**, *12*, 951–960.
- (17) Chen, S.-F.; Liu, Y.-J.; Navizet, I.; Ferré, N.; Fang, W.-H.; Lindh, R. *J. Chem. Theory Comput.* **2011**, *7*, 798–803.
- (18) Song, C.-I.; Rhee, Y. M. *J. Am. Chem. Soc.* **2011**, *133*, 12040–12049.
- (19) Nakatsu, T.; Ichiyama, Y.; Hiratake, J.; Saldanha, A.; Kobashi, N.; Sakata, K.; Kato, H. *Nature* **2006**, *440*, 372–376.
- (20) Pinto da Silva, L.; Esteves da Silva, J. C. G. *J. Comput. Chem.* **2011**, *32*, 2654–2663.
- (21) Min, C. G.; Ren, A. M.; Guo, J. F.; Li, Z. W.; Zou, L. Y.; Goddard, J. D.; Feng, J. K. *ChemPhysChem* **2010**, *11*, 251–259.
- (22) Min, C. G.; Ren, A. M.; Guo, J. F.; Zou, L. Y.; Goddard, J. D.; Sun, C. C. *ChemPhysChem* **2011**, *11*, 2199–2204.
- (23) Liu, Y. J.; De Vico, L.; Lindh, R. *J. Photochem. Photobiol., A* **2008**, *194*, 261–267.
- (24) Chen, S. F.; Yue, L.; Liu, Y. J.; Lindh, R. *Int. J. Quantum Chem.* **2011**, *111*, 3371.
- (25) Pinto da Silva, L.; Esteves da Silva, J. C. G. *ChemPhysChem* **2011**, *12*, 3002–3008.
- (26) Navizet, I.; Liu, Y. J.; Ferré, N.; Fang, W. H.; Lindh, R. *J. Am. Chem. Soc.* **2010**, *132*, 706–712.
- (27) Milne, B. F.; Marques, M. A.; Nogueira, F. *Phys. Chem. Chem. Phys.* **2010**, *12*, 14285–14293.
- (28) Naumov, P.; Ozawa, Y.; Ohkubo, K.; Fukuzumi, S. *J. Am. Chem. Soc.* **2009**, *131*, 11590–11605.
- (29) Cai, D.; Marques, M. A.; Nogueira, F. *J. Phys. Chem. B* **2011**, *115*, 329.
- (30) Nakatani, N.; Hasegawa, J.-Y.; Nakatsuji, H. *J. Am. Chem. Soc.* **2007**, *129*, 8756–8765.
- (31) Song, C. I.; Rhee, Y. M. *Int. J. Quantum Chem.* **2011**, *111*, 4091–4105.
- (32) Auld, D. S.; Lovell, S.; Thorne, N.; Lea, W. A.; Maloney, D. J.; Shen, M.; Rai, G.; Battaile, K. P.; Thomas, C. J.; Simeonov, A.; et al. *Proc. Natl. Acad. Sci. U.S.A.* **2010**, *107*, 4878–4883.
- (33) Naumov, P.; Kochunnonny, M. *J. Am. Chem. Soc.* **2010**, *132*, 11566–11579.

- (34) Case, D. A.; Cheatham, T. E.; Darden, T.; Gohlke, H.; Luo, R.; Merz, K. M.; Onufriev, A.; Simmelring, C.; Wang, B.; Wodds, R. J. *Comput. Chem.* **2005**, *26*, 1668–1688.
- (35) Duan, Y.; Wu, C.; Chowdhury, S.; Lee, M. C.; Xiong, G. M.; Zhang, W.; Yang, R.; Cieplak, P.; Luo, R.; Lee, T.; et al. *J. Comput. Chem.* **2003**, *24*, 1999–2012.
- (36) Cramer, C. J. *Essentials of Computational Chemistry*; Wiley: New York, 2002; p 153.
- (37) Foresman, J. B.; Head-Gordon, M.; Pople, J. A.; Frisch, M. J. *J. Phys. Chem.* **1992**, *96*, 135–149.
- (38) Wang, J. M.; Wolf, R. M.; Caldwell, J. W.; Kollman, P. A.; Case, D. A. *J. Comput. Chem.* **2004**, *25*, 1157–1174.
- (39) Morris, G. M.; Huey, R.; Lindstrom, W.; Sanner, M. F.; Belew, R. K.; Goddard, D. S.; Olsen, A. J. *J. Comput. Chem.* **2009**, *30*, 2785–2791.
- (40) Phillips, J. C.; Braun, R.; Wang, W.; Gumbart, J.; Tajkhorshid, E.; Villa, E.; Chipot, C.; Skellern, R. D.; Kale, L.; Schulten, K. *J. Comput. Chem.* **2005**, *26*, 1781–1802.
- (41) Essmann, U.; Perera, L.; Berkowitz, M. L.; Darden, T.; Lee, H.; Pedersen, L. G. *J. Chem. Phys.* **1995**, *103*, 8577–8593.
- (42) Gross, E. K. U.; Kohn, W. *Adv. Quantum Chem.* **1990**, *21*, 255–291.
- (43) Casida, M. E. *Recent Advances in Density Functional Methods*; World Scientific: Singapore, 1995.
- (44) Adamo, C.; Barone, V. *J. Chem. Phys.* **1999**, *110*, 6158–6170.
- (45) Yang, T.; Goddard, J. D. *J. Phys. Chem. A* **2007**, *111*, 4489–4497.
- (46) Fujimoto, K.; Hayashi, S.; Hasegawa, J.-Y.; Nakatsuji, H. *J. Chem. Theory Comput.* **2007**, *3*, 605–618.
- (47) Li, Z.-W.; Ren, A.-M.; Guo, J.-F.; Yang, T.; Goddard, J. D.; Feng, J.-K. *J. Phys. Chem. A* **2008**, 9796–9800.
- (48) Barone, V.; Cossi, M. *J. Phys. Chem. A* **1998**, *102*, 1995–2001.
- (49) Frisch, M. J.; Trucks, G. W.; Schlegel, H. B.; Scuseria, G. E.; Robb, M. A.; Cheeseman, J. R.; Montgomery, J. A., Jr.; Vreven, T.; Kudin, K. N.; Burant, J. C.; et al. *Gaussian 03*, revision C.02; Gaussian, Inc.: Wallingford, CT, 2004.
- (50) Roca-Sanjuán, D.; Delcey, M.; Navizet, I.; Ferré, N.; Liu, Y. J.; Lindh, R. *J. Chem. Theory Comput.* **2011**, *7*, 4060–4069.